

Neha U. Parsekar, Kedar U. Narvekar and Bikshandarkoil R. Srinivasan*

Synthesis and structural characterization of three new mixed ligand alkaline-earth metal picrates

<https://doi.org/10.1515/znb-2022-0003>

Received January 7, 2022; accepted January 10, 2022;
published online January 31, 2022

Abstract: The dissolution of alkaline-earth metal carbonate in aqueous picric acid followed by reaction with nicotinamide results in the formation of $[M(H_2O)_n(nic)_2(pic)_2]$ ($nic = \text{nicotinamide}$; $pic = \text{picrate}$; $n = 1$ and $M = \text{Ba 1}$; $n = 2$ and $M = \text{Ca (or Sr) 2 (or 3)}$). In $[Ba(H_2O)(nic)_2(pic)_2]$ **1**, the barium and the oxygen atoms of a terminal aqua ligand are located on a two-fold axis. Compound **1** exhibits a $\{\text{BaO}_2\text{N}_2\}$ coordination sphere, where the barium atom is bonded to a unique bidentate picrate and the crystallographically independent nicotinamide bridges to two symmetry related barium atoms with a $\text{Ba}\cdots\text{Ba}$ separation of 9.799 \AA via the pyridine nitrogen and the amide oxygen atoms leading to the formation of a two-dimensional coordination polymer. The compounds **2** and **3** are isostructural with discrete molecules. The central Ca atom in **2** (or Sr in **3**) located on a two-fold axis is bonded to a crystallographically unique terminal aqua ligand, an independent monodentate nicotinamide and a unique bidentate picrate anion resulting in a distorted $\{\text{MO}_8\}$ polyhedron. The mixed ligand alkaline-earth metal picrates **1–3** exhibit three varieties of hydrogen bonding and $\pi\cdots\pi$ stacking interactions. Several alkaline-earth metal picrates are compared in this study.

Keywords: alkaline-earth metal; barium coordination polymer; calcium; nicotinamide; picrate; strontium.

Dedicated to Professor Christian Näther on the occasion of his 60th birthday.

1 Introduction

The past two decades have witnessed a rapid growth of publications in the area of alkaline-earth metal chemistry. Synthetic methodologies, crystal structures, important properties and related applications of alkaline-earth metal

compounds are described in a recent review article titled, “*Chemistry of alkaline earth metals: It is not all ionic and definitely not boring!*” by Fromm [1]. The relevance of the present work on the mixed ligand alkaline-earth metal picrates can be evidenced by the following statement from Fromm’s review which is quoted verbatim “*While magnesium and calcium are the best studied among the alkaline earth metal compounds, the heavier alkaline earth metals have not yet been studied in detail, and recent results show the potential progress to be done*” [1].

Several research groups are currently investigating alkaline-earth based materials with a view to unravel the rich chemistry of the structurally flexible alkaline-earths [2–15]. The lighter element Be (which is known to be toxic) adopts mainly a tetrahedral coordination, while the biologically important Mg is known to prefer hexa-coordination in a majority of its compounds. In contrast, the heavier congeners namely Ca, Sr and Ba are structurally flexible and exhibit variable coordination numbers as evidenced by several structurally characterized alkaline-earth materials listed in the Cambridge Structural Database (CSD) [16].

A variety of synthetic methods including hydrothermal/solvothermal, mechanochemical, sonochemical processes etc. have been employed for compound preparation [17–25]. In our alkaline-earth metal chemistry research program, we have employed an aqueous reaction protocol, which involves the dissolution of alkaline-earth metal carbonates by reaction with an acidic ligand. For this purpose, we have chosen the readily available nitroaromatics as acidic ligands and have developed an extensive chemistry of alkaline-earth metal 4-nitrobenzoates [26–36]. We have demonstrated that coligands like dimethylformamide, *N*-methylformamide etc. can be incorporated in the coordination sphere of the alkaline-earth metals under ambient conditions resulting in the formation of coordination polymers which exhibit very short M–O(amide) ($M = \text{alkaline-earth metal}$) bonds [37–39]. We have extended these studies using picric acid (picH , for 2,4,6-trinitrophenol) for dissolution of metal carbonate and reported on the structure characterization of a barium coordination polymer containing a μ_2 -tetradentate bridging picrate [40]. The neutral molecule nicotinamide (nic) also known as niacinamide is a biologically important compound [41] and has been chosen as a coligand in the present study of the $\text{MCO}_3/\text{picH}/\text{H}_2\text{O}$

*Corresponding author: Bikshandarkoil R. Srinivasan, School of Chemical Sciences, Goa University, Goa 403206, India,
E-mail: sriini@unigoa.ac.in. <https://orcid.org/0000-0002-6598-6726>

Neha U. Parsekar and Kedar U. Narvekar, School of Chemical Sciences, Goa University, Goa 403206, India

reaction system. The details of the syntheses, vibrational spectra and crystal structures of three new mixed ligand alkaline-earth metal picrates $[M(H_2O)_n(nic)_2(pic)_2]$ ($n = 1$ and $M = Ba$ **1**; $n = 2$ and $M = Ca$ (or Sr) **2** or **3**) are described in this report.

2 Experimental

2.1 Materials and methods

All chemicals were used as received from commercial sources without any further purification. Infrared (IR) spectra of the solid samples taken up in KBr pellets were recorded on a Shimadzu (IR Prestige-21) FT-IR spectrometer in the range $4000\text{--}400\text{ cm}^{-1}$ at a resolution of 4 cm^{-1} . Raman spectra of the solids and their aqueous solutions were measured by using an Agilent PeakSeeker Pro Raman instrument with 785 nm laser irradiation and a laser power of 100 mW . X-ray powder patterns were recorded, on a Rigaku Miniflex II powder diffractometer using Cu-K α radiation with a Ni filter. For single crystal structure determination, X-ray intensity data was collected on a Bruker D8 Quest Eco X-ray

diffractometer, using graphite-monochromated Mo-K α radiation. The structures were solved with Direct Methods using SHELXS-97 [42] and refinement was carried out against F^2 using SHELXL-2016 [42]. All non-hydrogen atoms were refined anisotropically. The H atoms bonded to the aromatic carbon atoms and the H atoms of the amide nitrogen atoms were located in difference maps but were positioned with idealized geometry and refined isotropically with $U_{iso}(H) = 1.2 U_{eq}(C,N)$ using a riding model. The O-H hydrogen atoms were located in difference maps, and were refined using a riding model. Technical details of data acquisition and selected refinement results for **1**–**3** are given in Table 1.

2.2 Synthesis of $[M(H_2O)_n(nic)_2(pic)_2]$ ($n = 1$ and $M = Ba$ **1**; $n = 2$ and $M = Ca$ (or Sr) **2** or **3**)

Picric acid (picH) is known to be an explosive chemical. In view of this, it is quite essential to follow appropriate safety regulations in the handling, storage and disposal of picric acid and compounds derived from it. In this study, all experiments were performed on a gram scale of picric acid. A mixture of $BaCO_3$ (0.395 g, 2 mmol) and picH (0.916 g, 4 mmol) was taken up in water ($\sim 30\text{ mL}$) to obtain a slurry. The slurry was stirred well and brisk effervescence could be observed accompanied by the formation of a yellow solution. Slow warming of the

Table 1: Crystal data and structure refinement for **1**–**3**.

| Refinement result | Compound 1 | Compound 2 | Compound 3 |
|--------------------------------------------|----------------------------------------------------------------------|----------------------------------------------------------------------|----------------------------------------------------------------------|
| Empirical formula | $C_{24}H_{18}BaN_{10}O_{17}$ | $C_{24}H_{20}CaN_{10}O_{18}$ | $C_{24}H_{20}N_{10}O_{18}Sr$ |
| Formula weight (g mol $^{-1}$) | 855.82 | 776.58 | 824.12 |
| Temperature (K) | 293(2) | 293(2) | 293(2) |
| Wavelength (Å) | 0.71073 | 0.71073 | 0.71073 |
| Crystal system | Monoclinic | Monoclinic | Monoclinic |
| Space group | $C2/c$ | $C2/c$ | $C2/c$ |
| Unit cell dimensions | | | |
| a (Å) | 16.3113(5) | 27.2850(17) | 26.985(3) |
| b (Å) | 10.8621(4) | 9.8636(6) | 10.0221(12) |
| c (Å) | 18.1809(6) | 12.5517(8) | 12.6504(15) |
| β (°) | 105.0960(10) | 113.627(2) | 111.810(4) |
| Volume (Å 3) | 3110.04(18) | 3094.9(3) | 3176.4(7) |
| Z | 4 | 4 | 4 |
| D_{calc} (g cm $^{-3}$) | 1.83 | 1.67 | 1.72 |
| Absorption coefficient (mm $^{-1}$) | 1.4 | 0.3 | 1.8 |
| $F(000)$ (e) | 1696 | 1592 | 1664 |
| Crystal size (mm 3) | $0.40 \times 0.21 \times 0.12$ | $0.17 \times 0.13 \times 0.08$ | $0.21 \times 0.19 \times 0.14$ |
| θ range for data collection (°) | 2.587–27.131 | 3.037–28.311 | 2.975–28.324 |
| Limiting indices | $-20 \leq h \leq 20$ $-13 \leq k \leq 13$ $-23 \leq l \leq 23$ | $-36 \leq h \leq 35$ $-13 \leq k \leq 13$ $-14 \leq l \leq 16$ | $-36 \leq h \leq 24$ $-13 \leq k \leq 13$ $-16 \leq l \leq 13$ |
| Reflections collected/unique | 27075/3435 [$R(int) = 0.0215$] | 13381/3843 [$R(int) = 0.0427$] | 6637/3639 [$R(int) = 0.0349$] |
| Completeness $\theta = 25.242^\circ$ | 99.70 | 99.90 | 93.10 |
| Refinement method | Full-matrix least-squares on F^2 | | |
| Data/parameters | 3435/236 | 3843/246 | 3639/241 |
| Goodness of fit on F^2 | 1.081 | 1.04 | 1.047 |
| Final R indices [$I > 2\sigma(I)$] | $R1 = 0.0169$ $wR2 = 0.0432$ | $R1 = 0.0483$, $wR2 = 0.1007$ | $R1 = 0.0529$, $wR2 = 0.1212$ |
| R indices (all data) | $R1 = 0.0178$ $wR2 = 0.0440$ | $R1 = 0.0834$, $wR2 = 0.1158$ | $R1 = 0.0767$, $wR2 = 0.1317$ |
| Largest diff. peak and hole (e Å $^{-3}$) | 0.30 and -0.33 | 0.40 and -0.32 | 0.97 and -1.21 |
| CCDC deposition no | 2131550 | 2131551 | 2131552 |

reaction mixture on a water bath maintained at ~60 °C resulted in the formation of a clear, bright yellow solution after ~20 min. The pH was close to neutral and the reaction mixture was filtered into a clean beaker containing an aqueous solution of nicotinamide (0.244 g, 2 mmol; ~5 mL) and left undisturbed for crystallization. The yellow crystalline product was isolated by filtration, washed with ether and air-dried (yield: 1.22 g, 71%). The use of CaCO_3 (0.200 g, 2 mmol) or SrCO_3 (0.295 g, 2 mmol) instead of BaCO_3 afforded compounds **2** and **3** in good yields (1.08 g (78%) for **2** and 1.05 g for **3** (72%)).

Compound **1** IR data (KBr cm^{-1}): 3603(s), 3444(s), 3344(m), 3089(m), 1666(s), 1614(s), 1556(s), 1514(s), 1477(s), 1427(s), 1334(s), 1259(s), 1163(s), 1080(s), 1031(s), 968(w), 912(s), 831(m), 788(s), 744(m), 702(s), 642(w), 584(m), 518(w); Raman (cm^{-1}): 1554(w), 1333(s), 1309(s), 1159(w), 941(w), 823(m), 719(w).

Compound **2** IR data (KBr cm^{-1}): 3626(s), 3469(s), 3323–2500(br), 1693(s), 1612(s), 1565(s), 1514(w), 1487(w), 1429(s), 1334(s), 1267(s), 1163(s), 1080(m), 1029(m), 939(m), 914(s), 835(w), 790(s), 744(s), 704(s), 642(m), 582(w), 522(m); Raman (cm^{-1}): 1554(w), 1314(s), 1164(w), 941(w), 823(m), 702(w).

Compound **3** IR data (KBr cm^{-1}): 3624(s), 3473(s), 3361–2500(br), 1693(s), 1614(s), 1568(s), 1514(w), 1487(w), 1427(s), 1363(m), 1334(s), 1261(s), 1161(s), 1080(m), 1029(m), 939(w), 912(s), 835(w), 790(s), 744(s), 704(s), 6940(m), 520(m); Raman (cm^{-1}): 1559(w), 1309(s), 1159(w), 941(w), 823(m), 702(w).

3 Results and discussion

3.1 Description of the crystal structures of compounds **1–3**

The three compounds (**1–3**) described in this study crystallize in the centrosymmetric monoclinic space group $C2/c$. The crystal structures consist of an alkaline-earth metal located on a two-fold axis, a terminal aqua ligand, a crystallographically independent picrate anion and a unique nicotinamide moiety. The geometric parameters of the organic ligands (Table S1) in **1–3** are in the normal range [16, 43]. In the monoqua compound $[\text{Ba}(\text{H}_2\text{O})(\text{nic})_2(\text{pic})_2]$ **1**, the barium atom and the oxygen atom O1 of the water molecule are situated on a two-fold axis.

The central Ba atom is bonded to a terminal aqua ligand (O1), two symmetry related picrate ligands via the phenolate (O3) and a nitro oxygen atom (O4), four symmetry related nicotinamide ligands via their amide oxygen atom (O2) and the pyridine nitrogen atom (N2) resulting in a $\{\text{BaO}_7\text{N}_2\}$ coordination polyhedron (Figure 1). The Ba–O/N bond lengths are scattered in a wide range between 2.6793(11) and 2.9329(14) Å (Table 2). The amide oxygen atom makes the shortest Ba1–O2 bond which is shorter than the Ba1–O3(phenolate) and Ba1–O1(aqua) bond lengths at 2.7107(12) and 2.834(2) Å, respectively. The nitro oxygen atom is involved in the longest Ba1–O4 distance of 2.9282(14) Å. The Ba–N distances are slightly longer

(Ba1–N2ⁱⁱ = 2.9329(14) Å) than the longest Ba–O distance. The distinct Ba–O/N bond lengths and O–Ba–O/N bond angles ranging from 56.38(4) to 151.66(6)° reveal that the tricapped trigonal prismatic $\{\text{BaO}_7\text{N}_2\}$ coordination polyhedron is quite distorted (Figure 2).

The O-donor aqua and picrate ligands are bound to the Ba atom in monodentate and bidentate fashion, respectively. In contrast, the unique nicotinamide functions as a (N, O) donor and bridges two symmetry related Ba cations separated by 9.799 Å (Figure 2). This bridging mode of nic via the amide oxygen and pyridine N atom organizes the Ba cations into a layer (Figure 3) in the crystallographic *ab* plane, resulting in the formation of a two-dimensional coordination polymer (Figure 3). In view of its special position, each Ba cation is bridged via a nic ligand to four symmetry related Ba cations and all Ba…Ba separations in the layer are identical.

Each Ba cation in the layer is further bonded to a terminal aqua and two symmetry related picrate ligands (Figure S1) accounting for the remaining five coordination sites. In view of the μ_2 -bridging coordination, the $\{\text{BaO}_7\text{N}_2\}$ polyhedra are discrete (Figure 4).

Unlike the monoqua compound **1**, which is a two-dimensional coordination polymer, the diaqua compounds $[\text{M}(\text{H}_2\text{O})_2(\text{nic})_2(\text{pic})_2]$ ($\text{M} = \text{Ca}$ (or Sr) **2** (or **3**)) are monomers and are isostructural. No pyridine N coordination is observed in **2** (or **3**). As in **1**, the water molecule and the

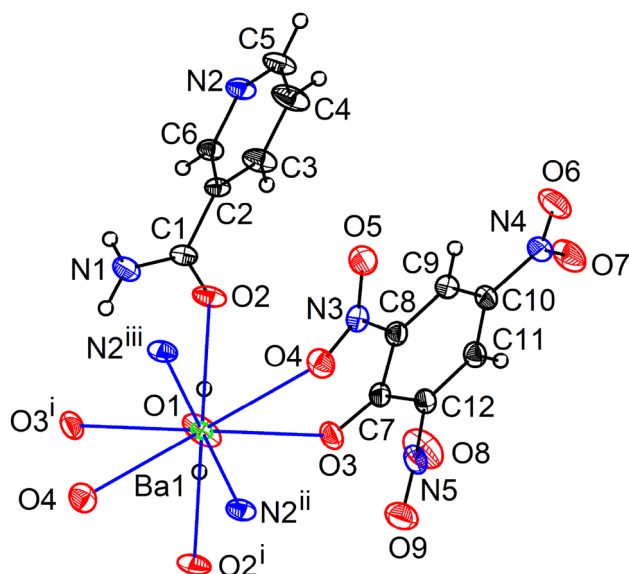


Figure 1: The asymmetric unit of **1** showing nine-fold coordination around the Ba atom. Displacement ellipsoids are drawn at the 30% probability level for all non-hydrogen atoms.
Symmetry code: (i) $-x+1, y, -z+3/2$ (ii) $x+1/2, y+1/2, z$ (iii) $-x+1/2, y+1/2, -z+3/2$.

Table 2: Selected geometric parameters for **1–3**.

| Bond lengths and bond angles (\AA , $^\circ$) of $\{\text{BaO}_7\text{N}_2\}$ and $\{\text{MO}_8\}$ polyhedra | | | |
|--------------------------------------------------------------------------------------------------------------------------|------------|-----------------------------------------|------------|
| $[\text{Ba}(\text{H}_2\text{O})(\text{nic})_2(\text{pic})_2]$ 1 | | | |
| Ba1–O2 | 2.6793(11) | Ba1–O4 ⁱ | 2.9281(14) |
| Ba1–O2 ⁱ | 2.6794(11) | Ba1–O4 | 2.9282(14) |
| Ba1–O3 | 2.7107(12) | Ba1–N2 ⁱⁱ | 2.9329(14) |
| Ba1–O3 ⁱ | 2.7107(12) | Ba1–N2 ⁱⁱⁱ | 2.9329(14) |
| Ba1–O1 | 2.834(2) | Ba ^{...} –Ba ^{iv} | 9.799 |
| O2–Ba1–O2 ⁱ | 151.66(6) | O3 ⁱ –Ba1–O4 | 150.79(4) |
| O2–Ba1–O3 | 83.84(5) | O1–Ba1–O4 | 115.31(3) |
| O2 ⁱ –Ba1–O3 | 85.67(4) | O4 ⁱ –Ba1–O4 | 129.37(5) |
| O2–Ba1–O3 ⁱ | 85.67(4) | O2–Ba1–N2 ⁱⁱ | 133.69(4) |
| O2 ⁱ –Ba1–O3 ⁱ | 83.84(5) | O2 ⁱ –Ba1–N2 ⁱⁱ | 72.95(4) |
| O3–Ba1–O3 ⁱ | 136.17(7) | O3–Ba1–N2 ⁱⁱ | 92.53(5) |
| O2–Ba1–O1 | 75.83(3) | O3 ⁱ –Ba1–N2 ⁱⁱ | 124.20(4) |
| O2 ⁱ –Ba1–O1 | 75.83(3) | O1–Ba1–N2 ⁱⁱ | 144.30(3) |
| O3–Ba1–O1 | 68.09(3) | O4 ⁱ –Ba1–N2 ⁱⁱ | 67.89(4) |
| O3 ⁱ –Ba1–O1 | 68.08(3) | O4–Ba1–N2 ⁱⁱ | 71.45(4) |
| O2–Ba1–O4 ⁱ | 125.37(4) | O2–Ba1–N2 ⁱⁱⁱ | 72.95(4) |
| O2 ⁱ –Ba1–O4 ⁱ | 68.32(4) | O2 ⁱ –Ba1–N2 ⁱⁱⁱ | 133.69(4) |
| O3–Ba1–O4 ⁱ | 150.79(4) | O3–Ba1–N2 ⁱⁱⁱ | 124.20(4) |
| O3 ⁱ –Ba1–O4 ⁱ | 56.38(4) | O3 ⁱ –Ba1–N2 ⁱⁱⁱ | 92.53(5) |
| O1–Ba1–O4 ⁱ | 115.31(3) | O1–Ba1–N2 ⁱⁱⁱ | 144.30(3) |
| O2–Ba1–O4 | 68.31(4) | O4 ⁱ –Ba1–N2 ⁱⁱⁱ | 71.45(4) |
| O2 ⁱ –Ba1–O4 | 125.37(4) | O4–Ba1–N2 ⁱⁱⁱ | 67.89(4) |
| O3–Ba1–O4 | 56.38(4) | N2 ⁱⁱ –Ba1–N2 ⁱⁱⁱ | 71.40(6) |
| $[\text{Ca}(\text{H}_2\text{O})_2(\text{nic})_2(\text{pic})_2]$ 2 | | | |
| Ca1–O2 | 2.3578(16) | Ca1–O1 | 2.4141(17) |
| Ca1–O2 ⁱ | 2.3578(16) | Ca1–O1 ⁱ | 2.4141(17) |
| Ca1–O3 | 2.3916(14) | Ca1–O4 ⁱ | 2.5391(17) |
| Ca1–O3 ⁱ | 2.3916(14) | Ca1–O4 | 2.5391(17) |
| O2–Ca1–O2 ⁱ | 78.94(8) | O1–Ca1–O1 ⁱ | 138.07(9) |
| O2–Ca1–O3 | 80.10(6) | O2–Ca1–O4 ⁱ | 122.67(6) |
| O2 ⁱ –Ca1–O3 | 84.07(6) | O2 ⁱ –Ca1–O4 ⁱ | 135.00(5) |
| O2–Ca1–O3 ⁱ | 84.07(6) | O3–Ca1–O4 ⁱ | 134.56(6) |
| O2 ⁱ –Ca1–O3 ⁱ | 80.10(6) | O3 ⁱ –Ca1–O4 ⁱ | 65.57(5) |
| O3–Ca1–O3 ⁱ | 159.46(8) | O1–Ca1–O4 ⁱ | 76.80(6) |
| O2–Ca1–O1 | 149.98(6) | O1 ⁱ –Ca1–O4 ⁱ | 69.54(6) |
| O2 ⁱ –Ca1–O1 | 71.73(6) | O2–Ca1–O4 | 135.00(5) |
| O3–Ca1–O1 | 102.66(6) | O2 ⁱ –Ca1–O4 | 122.67(6) |
| O3 ⁱ –Ca1–O1 | 84.75(6) | O3–Ca1–O4 | 65.57(5) |
| O2–Ca1–O1 ⁱ | 71.73(6) | O3 ⁱ –Ca1–O4 | 134.56(6) |
| O2 ⁱ –Ca1–O1 ⁱ | 149.98(6) | O1–Ca1–O4 | 69.54(6) |
| O3–Ca1–O1 ⁱ | 84.75(6) | O1 ⁱ –Ca1–O4 | 76.80(6) |

Table 2: (continued)

| Bond lengths and bond angles (\AA , $^\circ$) of $\{\text{BaO}_7\text{N}_2\}$ and $\{\text{MO}_8\}$ polyhedra | | | |
|--------------------------------------------------------------------------------------------------------------------------|------------|--------------------------------------|------------|
| O3 ⁱ –Ca1–O1 ⁱ | 102.66(6) | O4 ⁱ –Ca1–O4 | 72.27(8) |
| [Sr(H ₂ O) ₂ (nic) ₂ (pic) ₂] 3 | | | |
| Sr1–O2 | 2.481(3) | Sr1–O1 ⁱ | 2.553(3) |
| Sr1–O2 ⁱ | 2.481(3) | Sr1–O1 | 2.553(3) |
| Sr1–O3 ⁱ | 2.514(2) | Sr1–O4 | 2.648(3) |
| Sr1–O3 | 2.514(2) | Sr1–O4 ⁱ | 2.648(3) |
| O2–Sr1–O2 ⁱ | 78.75(14) | O1 ⁱ –Sr1–O1 | 138.23(12) |
| O2–Sr1–O3 ⁱ | 82.01(9) | O2–Sr1–O4 | 137.23(8) |
| O2 ⁱ –Sr1–O3 ⁱ | 84.04(9) | O2 ⁱ –Sr1–O4 | 118.73(10) |
| O2–Sr1–O3 | 84.04(9) | O3 ⁱ –Sr1–O4 | 134.98(8) |
| O2 ⁱ –Sr1–O3 | 82.01(9) | O3–Sr1–O4 | 62.61(8) |
| O3 ⁱ –Sr1–O3 | 161.93(11) | O1i–Sr1–O4 | 77.05(9) |
| O2–Sr1–O1 ⁱ | 72.46(9) | O1–Sr1–O4 | 70.37(8) |
| O2 ⁱ –Sr1–O1 ⁱ | 148.47(9) | O2–Sr1–O4 ⁱ | 118.73(10) |
| O3 ⁱ –Sr1–O1 ⁱ | 104.04(9) | O2 ⁱ –Sr1–O4 ⁱ | 137.23(8) |
| O3–Sr1–O1 ⁱ | 82.49(9) | O3 ⁱ –Sr1–O4 ⁱ | 62.61(8) |
| O3–Sr1–O1 | 104.05(9) | O4–Sr1–O4 ⁱ | 76.42(12) |

Symmetry transformations used to generate equivalent atoms:

Symmetry code for **1**: (i) $-x+1, y, -z+3/2$ (ii) $x+1/2, y+1/2, z$ (iii) $-x+1/2, y+1/2, -z+3/2$ (iv) $x-1/2, y-1/2, z$ for **2**: (i) $-x+1, y, -z+3/2$ for **3**: (i) $-x+1, y, -z+1/2$.

picrate anion function as monodentate and bidentate O-donor ligands, respectively. However, the nicotinamide in **2** (or **3**) functions as a monodentate O-donor ligand and is bonded to Ca (or Sr) atoms via the amide oxygen atom (O2) of the unique nicotinamide ligand resulting in a $\{\text{MO}_8\}$ coordination polyhedron (Figure 5, Figure S2). The absence of any bridging ligands in **2** (or **3**) explains their discrete nature.

The amide oxygen atom makes the shortest M–O2 bond ($\text{Ca1–O2} = 2.3578(16)$; $\text{Sr1–O2} = 2.481(3)$ \AA) while the nitro oxygen atom exhibits the longest M–O4 bond length ($\text{Ca1–O4} = 2.5391(17)$; $\text{Sr1–O4} = 2.648(3)$ \AA). The M–O3(phenoletate)

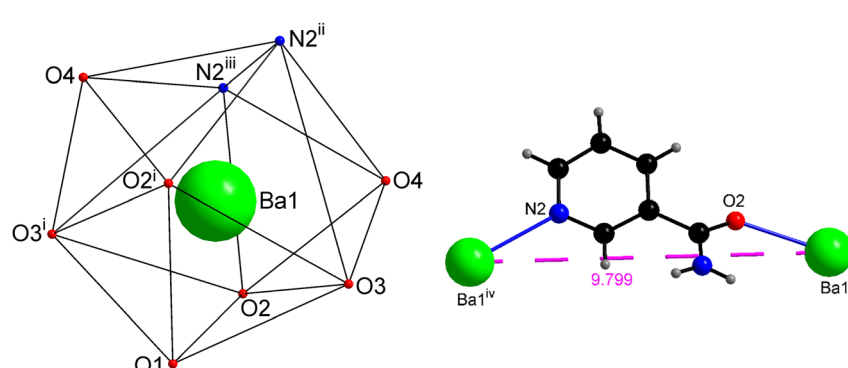


Figure 2: The distorted tricapped trigonal prismatic $\{\text{BaO}_7\text{N}_2\}$ coordination polyhedron (left). The (N, O) donor nic ligand bridges two symmetry related Ba cations (right). For symmetry code see Table 2.

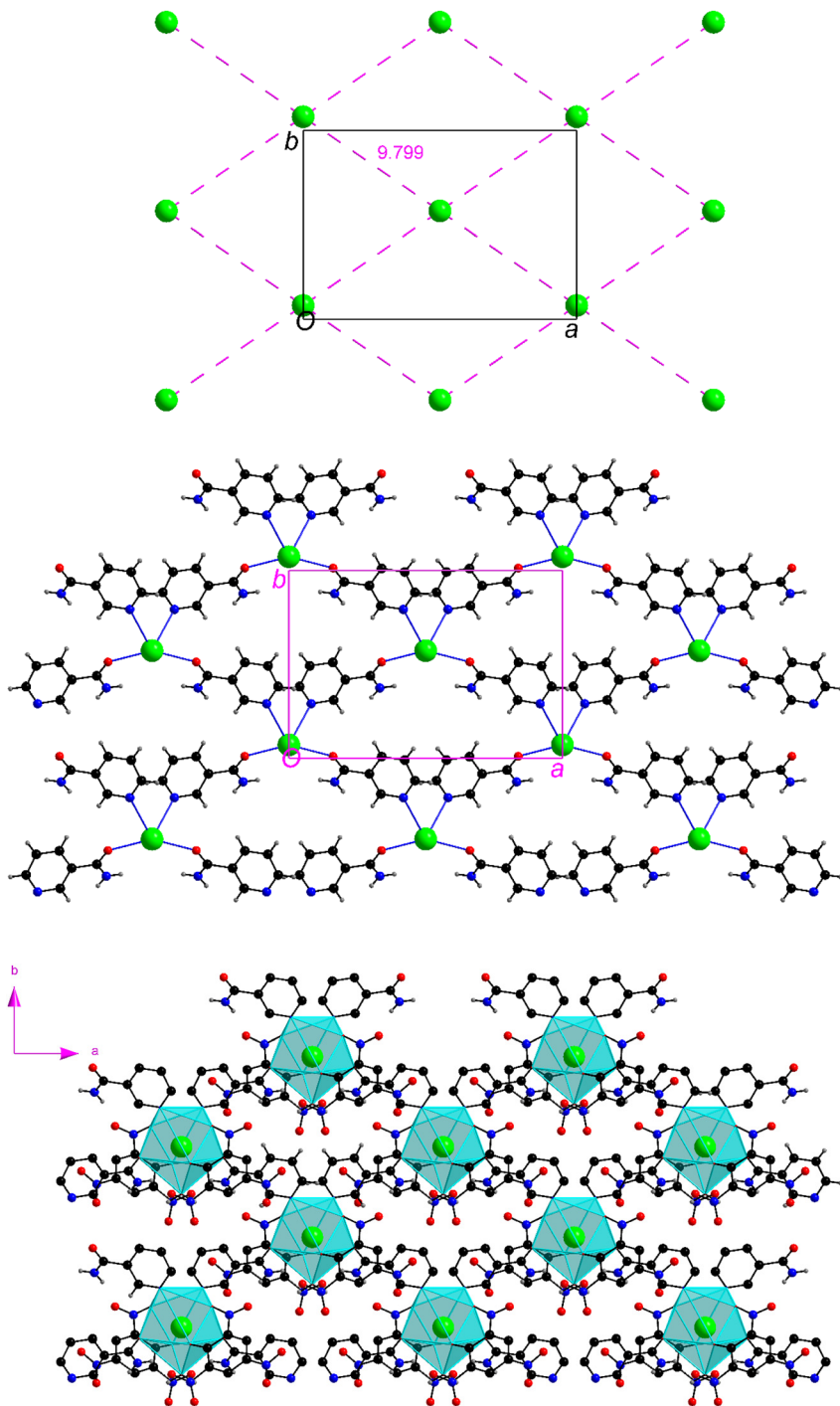


Figure 3: A portion of the layer of Ba cations in **1** (top). The same arrangement showing only bridging nic ligands (bottom). For clarity, terminal ligands around the Ba atoms (Figure S1) are not shown.

Figure 4: The discrete $\{\text{BaO}_7\text{N}_2\}$ polyhedra in **1**. For clarity, the H atoms of the aromatic ring are not shown.

and M–O1(aqua) distances in the isostructural molecules **2** and **3** are intermediate between the shortest and longest M–O bonds as in **1**, with the M–O4 bond slightly longer than M–O3 (Table 2). The distinct M–O bond lengths and a wide range of bond angles ($65.57(5)$ – $159.46(8)^\circ$ in **2**; $62.61(8)$ – $161.93(11)^\circ$ in **3**) indicate that the square-antiprismatic $\{\text{MO}_8\}$ coordination polyhedron is distorted (Figure S3). The amide oxygen atom is involved in the

shortest bond in the three compounds **1**–**3** described in this study. A similar observation has been made by us in our studies of alkaline-earth 4-nitrobenzoates [38–40].

In all three compounds **1**–**3**, the H atoms of the aqua ligands, the hydrogen atoms bonded to the nitrogen atom of the amine group of nic and the H atoms attached to the carbon atoms of the pyridine ring (C4, C5 and C6 in **1**; C6 in **2** (or **3**)) of the nic ligand function as H-donors, while the

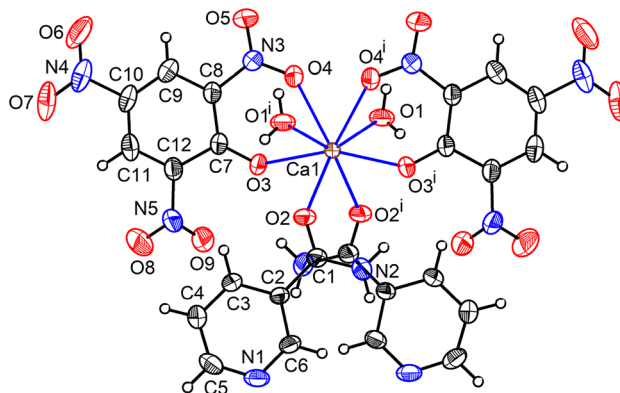


Figure 5: The crystal structure of **2** showing eight-fold coordination around the Ca atom. Displacement ellipsoids are drawn at 50% probability level for all the non-hydrogen atoms.

Symmetry code: (i) $-x+1, y, -z+3/2$. For the crystal structure of the isostructural **3** see Figure S2.

phenolate O (O3) and the oxygen atoms of the nitro groups of the picrate anion function as hydrogen bond acceptors resulting in three varieties of H-bonding interactions (Table S2). An analysis of the short ring interactions [44] in **1–3** was performed using the program Platon [45], to determine the ring centroid to ring centroid distances ($Cg \cdots Cg$) between adjacent aromatic rings. The values of these are found to be in the range 4.5669(2)–5.9138(2) Å in **1**, (3.5476(2)–5.2823(3) Å in **2** and 3.5435(4)–5.9676(7) Å in **3** (Table S3; Figures S4–S6). As it has been reported that stacking interactions between aromatic rings can exist at a very long $Cg \cdots Cg$ distances [46], the observed data reveal the presence of $\pi \cdots \pi$ stacking in crystals of **1–3**.

Several alkaline-earth metal picrates [47–54] have already been structurally characterized (Table 3). An analysis of these structures and their atomic coordinates available in the CSD reveals a rich structural chemistry of this group of compounds. The free ligand picric acid which crystallizes in the polar space group Pca_2_1 [55] forms several picrates, a majority of which crystallize in centrosymmetric space groups [16]. This trend can also be observed in alkaline-earth metal picrates. In addition to functioning as a charge balancing anion, the picrate anion is bonded to the alkaline-earth metal cations except for the case of $[Mg(H_2O)_6](pic)_2 \cdot 3H_2O$. In this compound containing an octahedral $[Mg(H_2O)_6]^{2+}$ moiety, the picrate is outside the coordination sphere of the cation. In $[Ca(H_2O)(teg)(pic)](pic) \cdot 3H_2O$ a picrate anion is not bonded to Ca cation while the second one is coordinated in a bidentate manner. The bidentate (η^2) binding mode of picrate, which involves the coordination of the phenolic oxygen atom and an oxygen atom of an ortho nitro group is observed in 12 of the 14 compounds in Table 3, especially in all the calcium picrates. Two barium picrates (entry no. 10, 11) containing two crystallographically unique picrates exhibit both monodentate (η^1) and bidentate binding modes (η^2).

A survey of the metal coordination polyhedra in these compounds reveals many interesting features. Ten of the compounds are bonded to only O-donor ligands while in four cases including **1**, coordination of N is observed. The Mg compound exhibits six-fold coordination while all Ca and Sr compounds exhibit eight-fold coordination. In the case of Ba the coordination number ranges from 8 (entry no. 10) to 11 in

Table 3: Binding mode of picrate units in alkaline-earth metal compounds.

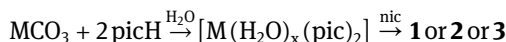
| No. | Compound | Space group | Coordination sphere | Binding mode of picrate | D ^a | Ref |
|-----|---------------------------------------|-------------|---------------------|-------------------------------------------------------------|----------------|-----------|
| 1 | $[Mg(H_2O)_6](pic)_2 \cdot 3H_2O$ | $P2_1/c$ | $\{MgO_6\}$ | uncoordinated | M ^b | [47] |
| 2 | $[Ca(H_2O)_4(pic)_2] \cdot H_2O$ | $Pmab$ | $\{CaO_8\}$ | bidentate (η^2 -O,O') | M ^b | [48] |
| 3 | $[Ca(H_2O)_4(pic)_2](L)$ | $C2/c$ | $\{CaO_8\}$ | bidentate (η^2 -O,O') | M ^b | [49] |
| 4 | $[Ca(bpy)_2(pic)_2]$ | $Pbca$ | $\{CaO_4N_4\}$ | bidentate (η^2 -O,O') | M ^b | [50] |
| 5 | $[Ca(H_2O)(teg)(pic)]pic^c$ | $P\bar{1}$ | $\{CaO_8\}$ | uncoordinated bidentate (η^2 -O,O') | | [51] |
| 6 | $[Ca(H_2O)_2(nic)_2(pic)_2]$ 2 | $C2/c$ | $\{CaO_8\}$ | bidentate (η^2 -O,O') | M ^b | This work |
| 7 | $[Sr(H_2O)_4(pic)_2] \cdot H_2O$ | $C2/c$ | $\{SrO_8\}$ | bidentate (η^2 -O,O') | 1D | [48] |
| 8 | $[Sr(H_2O)_2(nic)_2(pic)_2]$ 3 | $C2/c$ | $\{SrO_8\}$ | bidentate (η^2 -O,O') | M ^b | This work |
| 9 | $[Ba(H_2O)_2(pic)_2] \cdot H_2O^c$ | $P\bar{1}$ | $\{BaO_{10}\}$ | bidentate (η^2 -O,O') tridentate (μ_2 -O,O',O'') | 1D | [48] |
| 10 | $[Ba(ace)(phen)_2(pic)_2]^c$ | $Pbca$ | $\{BaO_4N_4\}$ | monodentate (η^1)bidentate (η^2 -O,O') | M ^b | [52] |
| 11 | $[Ba(H_2O)_2dbc(pic)_2]^c$ | $P\bar{1}$ | $\{BaO_{10}\}$ | monodentate (η^1)bidentate (η^2 -O,O') | M ^b | [53] |
| 12 | $[Ba(L_1)(pic)_2]$ | $P\bar{1}$ | $\{BaO_9N_2\}$ | bidentate (η^2 -O,O') | M ^b | [54] |
| 13 | $[Ba(DMSO)(pic)_2]$ | $P2_1/m$ | $\{BaO_{10}\}$ | tetridentate (μ_2 -O,O,O',O'') | 1D | [40] |
| 14 | $[Ba(H_2O)(nic)_2(pic)_2]$ 1 | $C2/c$ | $\{BaO_7N_2\}$ | bidentate (η^2 -O,O') | 2D | This work |

^aD = Dimensionality; ^bM = discrete monomer pic = picrate; L = 18-crown-6; bpy = 2,2'-Bipyridyl; teg = tetraethylene glycol; ace = acetone; phen = 1,10-phenanthroline; dbc = dibenzo-24-crown-8; L₁ = diaza 21-crown-7 ether; nic = nicotinamide; ^ctwo crystallographically unique picrates.

the Ba-picrate containing the diaza21-crown-7 ether (entry no. 12). A majority (10) of the compounds are discrete monomers which includes the single Mg-picrate and the picrates of Ca, while one Sr-picrate (entry no. 7) and three Ba picrates (entry no. 9, 13 and 14) are coordination polymers. The picrate ligand exhibits a μ_2 -tridentate and μ_2 -tetradentate bridging mode, respectively, in the water-rich $[\text{Ba}(\text{H}_2\text{O})_5(\text{pic})_2]\cdot\text{H}_2\text{O}$ (entry no. 9) and the anhydrous $[\text{Ba}(\text{DMSO})(\text{pic})]$ (entry no. 13) coordination polymers. The μ_2 -tridentate binding of picrate results in discrete $\{\text{BaO}_{10}\}$ polyhedra as in **1**, while the μ_2 -tetradentate binding of the unique picrate and the bridging DMSO ligand in $[\text{Ba}(\text{DMSO})(\text{pic})_2]$ results in the formation of a chain of face-sharing $\{\text{BaO}_{10}\}$ polyhedra flanked by the picrate ligands. In $[\text{Sr}(\text{H}_2\text{O})_4(\text{pic})_2]\cdot\text{H}_2\text{O}$ a bridging aqua ligand is responsible for the polymeric structure while in **1**, the neutral coligand nic is responsible for the two-dimensional structure. The monoqua Ba compound **1** is the only example of a two-dimensional coordination polymer in this series of compounds.

3.2 Synthetic aspects and spectral characteristics of **1–3**

The reaction of MCO_3 ($\text{M} = \text{Ca, Sr or Ba}$) with picric acid in water leads to a dissolution of the insoluble MCO_3 to afford water-rich metal picrates (entry nos. 2, 7 and 9 in Table 3) as documented in the literature [47, 48]. In recent work we have shown that solubilization of BaCO_3 in aqueous picric acid followed by reaction with DMSO results in the formation of the anhydrous compound $[\text{Ba}(\text{DMSO})(\text{pic})]$. In this study, the synthesis of compounds **1–3** was performed as shown below.



First, the insoluble metal carbonate was dissolved in aqueous picric acid by slow warming to obtain a yellow solution which was filtered. This was further reacted with nicotinamide to obtain **1–3** as yellow crystalline materials in good yield. The products thus obtained by slow evaporation of the reaction mixture were suitable for single crystal work. In the case of $\text{M} = \text{Mg}$, the above reaction resulted in the formation of a fine powder. A comparison of the experimental powder pattern of the bulk samples thus obtained with the theoretical pattern (Figures S7–S9) revealed that the materials are phase pure. The IR and Raman spectra of **1–3** (Figures S10 and S11) exhibit several bands which indicate the presence of the organic moieties. The IR bands at around 3600 and 3444 cm^{-1} in **1** can be assigned to the stretching vibrations of the water molecule(s) OH_2 and of the $-\text{NH}_2$ group of the amide,

respectively. The intense band at 1666 cm^{-1} in **1** can be assigned for the amide carbonyl vibration of nic which occurs at a lower energy compared to that of the free nic ligand which exhibits a strong signal at 1690 cm^{-1} . Pure picric acid exhibits a strong signal at 1190 cm^{-1} for the vibration of the C–O group and this occurs at 1160 cm^{-1} in **1–3**. The Raman spectra of all compounds exhibit an intense signal at $\sim 1309 \text{ cm}^{-1}$, which can be assigned for the symmetric stretching vibration of the nitro functionality.

4 Conclusions

The use of the neutral nicotinamide in the $\text{MCO}_3/\text{picH}/\text{H}_2\text{O}$ reaction system has resulted in the formation of three new mixed ligand alkaline-earth metal picrates **1–3**. The monoqua Ba compound $[\text{Ba}(\text{H}_2\text{O})(\text{nic})_2(\text{pic})_2]$ **1** is a two-dimensional coordination polymer, while the isostructural diaqua compounds $[\text{M}(\text{H}_2\text{O})_2(\text{nic})_2(\text{pic})_2]$ ($\text{M} = \text{Ca}$ **2**; $\text{M} = \text{Sr}$ **3**) are discrete monomers. A comparative study of several alkaline-earth metal picrates reveals intrinsic characteristics of the structural chemistry of this group of compounds.

5 Supporting information

Deposition numbers CCDC 2131550 (**1**), CCDC 2131551 (**2**) and CCDC 2131552 contain the supplementary crystallographic data for this paper. These data are provided free of charge by the joint Cambridge Crystallographic Data Centre and Fachinformationszentrum Karlsruhe Access Structures service www.ccdc.cam.ac.uk/structures. Supplementary Data (Figures S1–S11) and Tables (Tables S1–S3) associated with this article are available in electronic form.

Author contributions: All the authors have accepted responsibility for the entire content of this submitted manuscript and approved submission.

Research funding: Financial assistance was provided to the School of Chemical Sciences (formerly Department of Chemistry), Goa University at the level of DSA-I under the Special Assistance Programme (SAP) by the University Grants Commission, New Delhi.

Conflict of interest statement: The authors declare no conflicts of interest regarding this article.

References

- Fromm K. M. Chemistry of alkaline earth metals: it is not all ionic and definitely not boring. *Coord. Chem. Rev.* 2020, **408**, 213193–213214.

2. Fromm K. M., Gueneau E. D. Structures of alkali and alkaline earth metal clusters with oxygen donor ligands. *Polyhedron* 2004, **23**, 1479–1504.
3. Fromm K. M. Coordination polymer networks with s-block metal ions. *Coord. Chem. Rev.* 2008, **252**, 856–885.
4. Datta S., Gamer M. T., Roesky P. W. Aminotroponiminate calcium and strontium complexes. *Dalton Trans.* 2008, 2839–2843; <https://doi.org/10.1039/b719552d>.
5. Banerjee D., Parise J. B. Recent advances in s-block metal carboxylate networks. *Cryst. Growth Des.* 2011, **11**, 4704–4720.
6. Arlin J. B., Florence A. J., Johnston A., Kennedy A. R., Miller G. J., Patterson K. Systematic data set for structure-property investigations: solubility and solid-state structure of alkaline earth metal salts of benzoates. *Cryst. Growth Des.* 2011, **11**, 1318–1327.
7. Banerjee D., Zhang Z., Plonka A. M., Li J., Parise J. B. A calcium coordination framework having permanent porosity and high CO₂/N₂ selectivity. *Cryst. Growth Des.* 2012, **12**, 2162–2165.
8. Foo M. L., Horike S., Inubushi Y., Kitagawa S. An alkaline earth I³⁺⁰ porous coordination polymer: [Ba₂TMA(NO₃)(DMF)]. *Angew. Chem. Int. Ed.* 2012, **51**, 6107–6111.
9. Foo M. L., Horike S., Duan J., Chen W., Kitagawa S. Tuning the dimensionality of inorganic connectivity in barium coordination polymers via biphenyl carboxylic acid ligands. *Cryst. Growth Des.* 2013, **13**, 2965–2972.
10. Chanthaphally A., Quah H. S., Vittal J. J. Solid-state reactivity of supramolecular isomers: a study of the s-block coordination polymers. *Cryst. Growth Des.* 2014, **14**, 2605–2613.
11. Bauer H., Thum K., Alonso M., Fischer C., Harder S. Alkene transfer hydrogenation with alkaline-earth metal catalysts. *Angew. Chem. Int. Ed.* 2016, **55**, 4248–4253.
12. Balendra, Banday A., Murugavel S., Kanaujia P. K., Prakash G. V., Ramanan A. Calcium and strontium coordination polymers based on rigid and flexible aromatic dicarboxylates: synthesis, structure, photoluminescence and dielectric properties. *ChemistrySelect* 2017, **2**, 8567–8576.
13. Georg P., Das R. K., Chowdhury P. Facile microwave synthesis of Ca-BDC metal organic framework for adsorption and controlled release of Curcumin. *Microporous Mesoporous Mater.* 2019, **281**, 161–171.
14. Balendra, Banday M., Tewari S., Singh B., Murugavel S., Ramanan A. Alkaline-earth metal based coordination polymers assembled from two different V-shaped ligands: synthesis, structure, and dielectric properties. *Inorg. Chim. Acta* 2019, **495**, 118940.
15. Xian S., Lin Y., Wang H., Li J. Calcium-based metal-organic frameworks and their potential applications. *Small* 2021, **17**, 2005165; <https://doi.org/10.1002/smll.202005165>.
16. Groom C. R., Bruno I. J., Lightfoot M. P., Ward S. C. The Cambridge structural database. *Acta Crystallogr.* 2016, **B72**, 171–179.
17. Dey C., Kundu T., Biswal B. P., Mallick A., Banerjee R. Crystalline metal-organic frameworks (MOFs): synthesis, structure and function. *Acta Crystallogr.* 2014, **B70**, 3–10.
18. Scholz G., Abdulkader A., Kemnitz E. Synthesis and crystal structure of two Cu^{II}-benzene-1,2,4,5-tetracarboxylates with three-dimensional open frameworks. *Z. Anorg. Allg. Chem.* 2014, **640**, 310–316.
19. Scholz G., Abdulkader A., Kemnitz E. Mechanochemical synthesis and characterization of alkaline earth metal terephthalates: M(C₈H₄O₄)·nH₂O (M = Ca, Sr, Ba). *Z. Anorg. Allg. Chem.* 2014, **640**, 317–324.
20. Al-Terkawi A. A., Scholz G., Emmerling F., Kemnitz E. Mechanochemical synthesis, characterization, and structure determination of new alkaline earth metal-tetrafluoroterephthalate frameworks: Ca(pBDC-F₄)·4H₂O, Sr(pBDC-F₄)·4H₂O, and Ba(pBDC-F₄). *Cryst. Growth Des.* 2016, **16**, 1923–1933.
21. Li T.-T., Cai S.-L., Zeng R.-H., Zheng S.-R. Structures and luminescent properties of two new main group coordination polymers based on 2-(hydroxymethyl)-1H-imidazole-4,5-dicarboxylic acid. *Inorg. Chem. Commun.* 2014, **48**, 40–43.
22. Halake S., Ok K. M. Crystal growth, differential gas adsorption, high thermal stability, and reversible coordination of two new barium-organic frameworks, Ba(SBA)(DMF)₄ and Ba₂(BTEC)(H₂O). *J. Solid State Chem.* 2015, **231**, 132–137.
23. Kelly N. R., Goetz S., Batten S. R., Kruger P. E. Coordination behaviour and network formation with 4,4',6,6'-tetracarboxy-2,2'-bipyridine and 4,4'-dicarboxy-2,2'-bipyridine ligands with rare and alkaline earth metals. *CrystEngComm* 2008, **10**, 68–78.
24. Moghzi F., Soleimannejad J. Sonochemical synthesis of a new nano-sized barium coordination polymer and its application as a heterogeneous catalyst towards sono-synthesis of biodiesel. *Ultrason. Sonochem.* 2018, **42**, 193–200.
25. Drzewiecka-Antonika A., Koziol A. E., Rejmak P., Lawniczak-Jablonska K., Nittlera L., Lisc T. Novel Ba(II) and Pb(II) coordination polymers based on citric acid: synthesis, crystal structure and DFT studies. *Polyhedron* 2017, **132**, 1–11.
26. Srinivasan B. R., Sawant S. C. Thermal and spectroscopic characterization of Mg(II) complexes of nitro-substituted benzoic acids. *Thermochim. Acta* 2003, **402**, 45–55.
27. Srinivasan B. R., Sawant J. V., Raghavaiah P. Synthesis, spectroscopy, thermal and X-ray structure studies of a seven coordinated hydrated Ca(II)-para-nitrobenzoate complex showing mono and bidentate carboxylate ligation. *Indian J. Chem.* 2006, **45A**, 2392–2399.
28. Srinivasan B. R., Sawant J. V., Nather C., Bensch W. Synthesis, spectroscopy and supramolecular structures of two magnesium 4-nitrobenzoate complexes. *J. Chem. Sci.* 2007, **119**, 243–252.
29. Srinivasan B. R., Raghavaiah P., Sawant J. V. Heptaqua(4-nitrobenzoato- κ_2 O,O')-strontium(II) 4-nitrobenzoate dehydrate. *Acta Crystallogr.* 2007, **E63**, m2251–m2252.
30. Srinivasan B. R., Sawant J. V., Raghavaiah P. Synthesis, spectroscopy, thermal studies and supramolecular structures of two new alkali-earth 4-nitrobenzoate complexes containing coordinated imidazole. *J. Chem. Sci.* 2007, **119**, 11–20.
31. Srinivasan B. R., Sawant J. V., Sawant S. C., Raghavaiah P. Catena-Poly[[[(pentaaqua)(4-nitrobenzoato-O,O')barium(II)] (μ -4-nitrobenzoato-O,O')]: a barium(II) coordination polymer showing O–H···O and C–H···O interactions. *J. Chem. Sci.* 2007, **119**, 593–601.
32. Srinivasan B. R., Shetgaonkar S. Y., Sawant J. V., Raghavaiah P. X-ray structure and properties of a calcium(II) coordination polymer showing μ_2 - η^1 : η^1 and μ_3 - η^2 : η^1 coordination modes of 4-nitrobenzoate. *Polyhedron* 2008, **27**, 3299–3305.
33. Srinivasan B. R., Shetgaonkar S. Y., Nather C., Bensch W. Solid state synthesis and characterization of a triple chain calcium(II) coordination polymer showing two different bridging

- 4-nitrobenzoate coordination modes. *Polyhedron* 2009, **28**, 534–540.
34. Srinivasan B. R., Shetgaonkar S. Y., Näther C. Preparation, crystal structures, and thermal studies of alkaline earth nitrocarboxylates. *Z. Anorg. Allg. Chem.* 2011, **637**, 130–136.
35. Srinivasan B. R., Shetgaonkar S. Y., Saxena M., Näther C. A new calcium(II) coordination polymer based on a μ_2 -bridging tridentate 4-nitrobenzoate. *Indian J. Chem.* 2012, **51A**, 435–443.
36. Srinivasan B. R., Raghavaiah P., Dhavskar K. T. Structural characterization of catena-[bis(μ -4-nitrobenzoato)-diaqua-calcium 4,4'-bipyridine] and catena-[bis(μ -4-nitrobenzoato)-diaqua-calcium 1H-1,2,4-triazole]. *Indian J. Chem.* 2021, **60A**, 785–796.
37. Srinivasan B. R., Dhavskar K. T. On the syntheses and structures of two calcium coordination polymers containing terminal amide ligands. *Indian J. Chem.* 2017, **56A**, 387–393.
38. Bhargao P. H., Srinivasan B. R. Synthesis and structural characterization of a barium coordination polymer based on a μ_2 -monoatomic bridging 4-nitrobenzoate. *J. Coord. Chem.* 2019, **72**, 2599–2615.
39. Parsekar N. U., Bhargao P. H., Näther C., Bensch W., Srinivasan B. R. Synthesis and structural characterization of three new strontium(II) coordination polymers based on 4-nitrobenzoate. *J. Inorg. Organomet. Polym. Mater.* 2021, **32**, 200–215.
40. Srinivasan B. R., Parsekar N. U., Narvekar K. U. Catena-poly(μ_2 -dimethylsulfoxide)bis(μ_2 -2,4,6-trinitrophenolato)barium(II). *IUCrData* 2020, **5**, x201498.
41. Mackay D., Hathcock J., Guarneri E. Niacin: chemical forms, bioavailability, and health effects. *Nutr. Rev.* 2012, **70**, 357–366.
42. Sheldrick G. M. Crystal structure refinement with SHELXL. *Acta Crystallogr.* 2015, **C71**, 3–8.
43. Srinivasan B. R., Parsekar N. U., Apreyan R. A., Petrosyan A. M. On the second harmonic generation activity in centrosymmetric crystals. *Mol. Cryst. Liq. Cryst.* 2019, **680**, 75–84.
44. Hunter C. A., Sanders J. K. M. The nature of π - π interactions. *J. Am. Chem. Soc.* 1990, **112**, 5525–5534.
45. Spek A. L. Structure validation in chemical crystallography. *Acta Crystallogr.* 2009, **D65**, 148–155.
46. Ninković D. B., Janjić G. V., Veljković D. Z., Sredojević D. N., Zarić S. D. What are the preferred horizontal displacements in parallel aromatic–aromatic interactions? Significant interactions at large displacements. *ChemPhysChem* 2011, **12**, 3511–3514.
47. Harrowfield J. M., Skelton B. W., White A. H. Structural studies of alkaline earth metal picrates. *Aust. J. Chem.* 1995, **48**, 1333–1347.
48. Diakiw V., Hambley T., Kepert D., Raston C., White A. Crystal structure of calcium picrate pentahydrate: a new eight-coordinate stereochemistry for [M(bidentate)₂(unidentate)₄]. *Aust. J. Chem.* 1979, **32**, 301–309.
49. Chekhlov A. N. *Koordinatsionna Khim.* 2001, **27**, 809.
50. Poonia N. S., Chandra R., Padmanabhan V. M., Yadav V. S. Coordination chemistry of alkali and alkaline earth cations: X-ray structural analysis of calcium(picrate)₂(2,2'-bipyridyl)₂. *J. Coord. Chem.* 1989, **21**, 167–174.
51. Singh T. P., Reinhardt R., Poonia N. S. Crystal & molecular structure of calcium (picrate)₂-tetraethylene glycol monohydrate. *Indian J. Chem.* 1984, **23A**, 976–982.
52. Postma R., Kanters J. A., Duisenberg A. J. M., Venkatasubramanian K., Poonia N. S. Structure of bis(10-phenanthroline)bis(2,4,6-trinitrophenolato)barium(II) acetone (1:1), [Ba(C₁₂H₈N₂)₂(C₆H₂N₃O₇)₂].C₃H₆O. *Acta Crystallogr.* 1983, **C39**, 1221–1225.
53. Hughes D. L., Wingfield J. N. Crystal structure of a complex showing simultaneous water-barium ion co-ordination to 6,7,9,10,12,13,20,21,23,24,26,27-dodecahydrodibenzo[b,n][1,4,7,10,13,16,19,22] octaoxacyclotetracosin (dibenzo-24-crown-8). *J. Chem. Soc. Chem. Commun.* 1977, 804–805; <https://doi.org/10.1039/c39770000804>.
54. Chandler C. J., Gable R. W., Gulbis J. M., Mackay M. F. Preparation and structural characterization of a diaza 21-crown-7 ether complex with barium picrate - (3,6,9,12,15-pentaoxa-26,29-diazatetracyclo[15.8.4.020,28.023,27]-nonaco sa-17,19,21,23,25(1),26,28-heptaene-2,16-dione)barium(II) picrate. *Aust. J. Chem.* 1988, **41**, 799–806.
55. Srikrishnan T., Soriano-Garcia M., Parthasarathy R. Orientation and intramolecular hydrogen bonding of nitro groups in the crystal structure of picric acid C₆H₃N₃O₇. *Z. Kristallogr.* 1980, **151**, 317–323.

Supplementary Material: The online version of this article offers supplementary material (<https://doi.org/10.1515/znb-2022-0003>).